IEEE Access
Multidisciplinary | Rapid Review | Open Access Journal

Received October 5, 2020, accepted October 28, 2020, date of publication November 3, 2020, date of current version November 12, 2020.

Digital Object Identifier 10.1109/ACCESS.2020.3035345

Melanoma Lesion Detection and Segmentation Using YOLOv4-DarkNet and Active Contour

SALEH ALBAHLI[1], NUDRAT NIDA[2,3], AUN IRTAZA[3,4], MUHAMMAD HAROON YOUSAF[3], (Senior Member, IEEE), AND MUHAMMAD TARIQ MAHMOOD[5], (Senior Member, IEEE)

[1]Department of Information Technology, College of Computer, Qassim University, Buraydah 51452, Saudi Arabia
[2]Department of Computer Science, Air University Islamabad, Aerospace and Aviation Campus, Kamra 43570, Pakistan
[3]Department of Computer Science, University of Engineering and Technology, Taxila 47050, Pakistan
[4]Department of Computer and Electrical Engineering, University of Michigan-Dearborn, Dearborn, MI 48128, USA
[5]School of Computer Science and Engineering, College of Future Convergence, Korea University of Technology and Education, Cheonan 31253, South Korea

Corresponding author: Muhammad Tariq Mahmood (tariq@koreatech.ac.kr)

We would like to thank the Deanship of Scientific Research, Qassim University for funding the publication of this project.

ABSTRACT Melanoma is the skin cancer caused by the ultraviolet radiation from the Sun and has only 15-20% of survival rate. Late diagnosis of melanoma leads to the severe malignancy of disease, and metastasis expands to the other body organs i.e. liver, lungs and brain. The dermatologists analyze the pigmented lesions over the skin to discriminate melanoma from other skin diseases. However, the imprecise analysis results in the form of a series of biopsies and it complicates the treatment. Meanwhile, the process of melanoma detection can be expedited through computer vision methods by analyzing the dermoscopic images automatically. However, the visual similarity between the normal and infected skin regions, and artifacts like gel bubbles, hair and clinical marks indicate low accuracy rates for these approaches. To overcome these challenges, in this article, a melanoma detection and segmentation approach is presented that brings significant improvement in terms of accuracy against state-of-the-art approaches. As a first step, the artifacts like hairs, gel bubbles, and clinical marks are removed from the dermoscopic images by applying the morphological operations, and image regions are sharpen. Afterwards, for infected region detection, we used YOLOv4 object detector by tuning it for melanoma detection to discriminate the highly correlated infected and non-infected regions. Once the bounding boxes against the melanoma regions are obtained, the infected melanoma regions are extracted by applying the active contour segmentation approach. For performance evaluation, the proposed approach is evaluated on ISIC2018 and ISIC2016 datasets and results are compared against state-of-the-art melanoma detection, and segmentation techniques. Our proposed approach achieves average dice score as 1 and Jaccard coefficient as 0.989. The segmentation result validates the practical bearing of our method in development of clinical decision support system for melanoma diagnosis in contrast to state-of-the-art methods. The YOLOv4 detector is capable to detect multiple skin diseases of same patient and multiple diseases of various patients.

INDEX TERMS Deep neural networks, skin cancer, skin lesion segmentation, active contour segmentation, CAD tool, melanoma localization, YOLOv4.

I. INTRODUCTION

Melanoma is the most lethal type of skin cancer that holds 9000 deaths counts around the world annually. Almost 2% of all skin cancer are melanoma, which is the cause of 75% mortality due to skin cancer [2]. The dermatologist conducts visual analysis to identify the clinical characteristic of melanoma lesion including, asymmetry, irregular borders, color variation, diameter greater than 6mm and evolving nature of mole for diagnosis. These indicative symptoms of melanoma are known as ABCDE rule, introduce by American Cancer Society [3]. However, manual diagnosis accuracy of ABCDE rule is 59-88% and still, the precise diagnosis decision relies on biopsy test for confirmation. Precise diagnosis

The associate editor coordinating the review of this manuscript and approving it for publication was Wei Liu.

of melanoma at earlier stages is desirable since melanoma is curable at earlier stages. At earlier stage melanoma is remediable through excision of melanoma affected lesion. However, manual diagnosis demands expert dermatologist, and even then, diagnosis decision suffers from subjective variation in observation and adversely affects the patient's life expectancy [4]. Therefore, the precise automatic melanoma diagnosis system is significant to facilitate the dermatologist in reliable diagnosis decision making and to reduce the series of unnecessary biopsies.

Dermoscopy imaging techniques are used to analyze the skin lesion at deeper level and improves the diagnosis of melanoma [5]. Although, dermoscopic images improve visual clarity, still precise recognition of melanoma from dermoscopic images is a challenging task due to wide variation in color, appearance, shape, and presence of artifacts including, hair, gel bubble, clinical rule marks (Figure 1). Several studies are presented to automate the analysis process of dermoscopic images and to extend the domain knowledge of melanoma recognition.

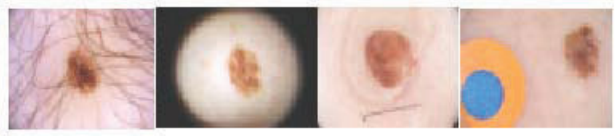

FIGURE 1. ISIC2018 dermoscopic images samples for melanoma lesion segmentation. Some natural and clinical artifacts are visible in sample images including, hair, black frame, gel bubble, clinical rule marks and color charts.

In the development of automatic melanoma recognition system, segmentation of melanoma effective lesions is a crucial process to improve the diagnostic performance. The automatic melanoma segmentation techniques can be categorized into traditional and deep learning techniques. The traditional techniques for melanoma segmentation includes Otsu's thresholding [6], adaptive thresholding [7], iterative stochastic region merging [8], iterative selection threshold [9], [10], and level set segmentation [11]. However, clinical or natural artifacts degrade the performance of threshold-based segmentation techniques [6]–[9]. The segmentation performance of Otsu's thresholding [6] is amenable, however boundaries of segmented region are irregular and it reduces the resolution of images. The limitation of Otsu's thresholding was overcome in [12] through averaging the intensities across the pixel. In [8], [13], melanoma lesion has been iteratively segmented by applying region merging algorithm that groups intensity-based similar regions. This technique is beneficial to overcome the challenges of low contrast, illumination variation and color imbalance in dermoscopic images, and it performs good segmentation of melanoma. The similar statistical attributes were used to segment the melanoma lesion [8]. However, stochastically region split and merge performance degraded when complex texture dermoscopic images are processed. Some techniques apply object detection algorithm on dermoscopic images to identify the melanoma affected regions that signify better segmentation results [14], [15]. In [14], the hyper-graph was used to map the saliency of melanoma region using super pixel information. Deep learning techniques [4], [5], [16]–[18] for melanoma segmentation have shown significant performance gain in contrast to traditional segmentation techniques. A fully convolutional residual network(FCRN) [4] was designed to overcome the issues of overfitting for deeper CNN models for melanoma segmentation. Recently, region based convolutional neural network(RCNN) [5] was applied to localize the melanoma lesion and later it segmented the lesion using fuzzy clustering. A 19 layered convolutional neural network [16] was developed to improve the segmentation of melanoma through estimating the Jaccard distance as loss function. The use of Jaccard distance as loss function in [16] resolves the class imbalance problem among the number of melanoma and normal skin pixels and improves the model learning. Melanoma lesion was segmented through full resolution convolutional network (FRCN) [18] that learns segmentation model through full spatial resolution features of dermoscopic images without preprocessing the images. Hybrid model was presented by combining the CNN model and recurrent neural network (RNN) to segment melanoma lesion and to overcome the natural and clinical artifacts in dermoscopic images [17]. However, two stage object detection models such as RCNN generate approximately 2000 region proposals per image for estimation of melanoma lesion; due to this melanoma localization becomes computationally expensive.

To overcome the computational overhead, we propose a three step process for melanoma segmentation which is the combination of skin refinement phase, melanoma localization phase, and segmentation phase. Initially, skin refinement step is effective to eliminate the unnecessary noisy objects like hairs, gel bubbles, clinical rule marks, and clinical charts, which is significant for precise segmentation of melanoma lesion. Then, we applied you look only once (YOLOv4) detector to localize the melanoma lesion as region of interest. After localization of melanoma, active contour segmentation technique was applied for segmentation of melanoma affected lesion. Our contributions can be summarized as follows:

1) Application of skin refinement step and YOLOv4 as melanoma detector. Our skin refinement step removes the unnecessary artifacts automatically, and we attribute it as one of the major factors for precise segmentation of melanoma lesions.
2) Our proposed method is capable to detect multiple melanoma lesions present in single image as well as multiple types of skin disease, and reduce the need of biopsy test for melanoma diagnosis.
3) Our active contour segmentation precisely segments the melanoma affected lesion and overcomes all the associated challenges exhibited within the ISIC2016 and ISIC2018 dermoscopic images dataset.
4) Experimental finding reveals the performance gain of our method in contrast to state-of-the-art methods,

which in turn validates the practical bearing of our proposed method in building a clinical decision support system for skin diseases.

II. PROPOSED METHOD

A. SYSTEM OVERVIEW

Consider the training-set as $\left(D^{(i)}, T^{(i)}\right)$, where $D^{(i)}$ are the dermoscopic images and $T^{(i)}$ are the corresponding melanoma lesion ground truth labels, and $i = \{1, 2, \ldots m\}$ represents the number of training samples. First of all, the training images are processed through the skin refinement phase to eliminate the hairs, tiny blood vessels, clinical rule marks, gel bubbles etc., and the visual quality of images is also enhanced. The corresponding refined images and their ground truth images are passed to the YOLOv4 [1] detector to learn melanoma lesion's deep representations; and to select melanoma affected skin regions. At test time, the learnt YOLOv4 [1] model uses deep feature representation from entire test dermoscopic image to differentiate between normal skin and melanoma affected lesion using regression operation and predicts bounding box across melanoma lesion. The localized melanoma lesion is processed further to segment out the lesion boundary through active contour segmentation. The architecture of the proposed method is presented in 2.

B. GENERATE GROUND TRUTH ANNOTATIONS

The ISIC2018 and ISIC2016 datasets consists of RGB dermoscopic images with corresponding binary mask images to represent the melanoma lesion in RGB images. For training YOLOv4 [1] requires both RGB dermoscopic images along with corresponding region as a training pairs. These training pairs are $\left(\hat{D}^{(i)}, T^{(i)}\right)$, where i represents the index of N training samples $i = \{1, 2, \ldots N\}$. We apply region split and merge segmentation on ground truth masks T, to extract the location of melanoma lesion to pass them to YOLOv4 for model learning.

C. SKIN ENHANCEMENT PHASE

Melanoma lesion segmentation is a challenging task due to presence of clinical or natural artifacts, including hairs, and clinical rule marks. Moreover, as the ISIC challenge dataset (details in section 3) comprises of dermoscopic images acquired through various dermoscopic cameras, therefore all images have high amount of variation in image contrast. Therefore, it is highly desirable to eliminate artifacts and enhance image quality to improve the melanoma localization and segmentation performance. To achieve this objective, we have applied morphological closing operations with two line structuring elements L_1, L_2 to mitigate the artifacts of clinical rule marks and hair, as expressed in (1) [5].

$$D^*(x, y) = (D(x, y) \oplus L_1) \ominus L_2 \tag{1}$$

The length of line structuring elements were chosen as ten pixels and direction of and to remove thick and thin hair. The morphological operations are applied on RGB coloured images, as we want colour, texture and shape information to generate a model for melanoma localization using YOLOv4 without any natural and clinical artefacts. For a given input color (RGB) image the morphological closing operation removes the hair from skin through line structuring elements S1. The closing operation performs dilation and then followed by erosion on RGB image with line structuring element. Whereas, the S1 consists of 10 pixels in direction of 90° and 180° against every pixel to obtained morphed image. After the application of morphological closing operation to eliminate hair and clinical rule marks, the resultant dermoscopic image becomes blurred. Therefore, sharpening operation is applied to enhance the edges of image by convolving unsharp filter over burred image $D^*(x, y)$ and generate an unsharp image $D(x, y)$. To obtain sharp dermoscopic image $\hat{D}(x, y)$, the un-sharp image $D(x, y)$ is subtracted from $D^*(x, y)$ dermoscopic image to sharpen the image edges, as illustrated in (2).

$$\hat{D}(x, y) = D^*(x, y) - D(x, y) \tag{2}$$

After skin enhancement phase, enhanced dermoscopic images are passed to the melanoma localization phase.

D. MELANOMA LOCALIZATION

Melanoma localization aims to identify the melanoma affected regions within the dermoscopic images. In proposed method, we have applied YOLOv4 deep neural network [1] for melanoma localization that transforms the detection task into regression problem. The detection of melanoma lesion using YOLOv4 has following attributes: precise melanoma lesion prediction, segregation of melanoma and normal skin class with prediction score, prediction across multiple scales. These factors empower YOLOv4 to detect melanoma at multiple resolutions.

The basic building block of YOLO detector family comprises of three parts including backbone, neck, and head component. The input images were processed through convolutional backbone network to describe the high level representation of melanoma based on colour, texture, and shape of melanoma lesion. The high level melanoma representation was down sampled to select deep features that generate stronger decision boundaries for melanoma prediction. At melanoma detection stage, multiple bounding boxes were generated and mapped across the dermoscopy image through aggregated convolutional backbone features in neck region of the detector. The head part of YOLO detector predicts the class melanoma and identify the location of melanoma lesion simultaneously.

The YOLO4 backbone model adapted for melanoma detection was cross stage partial network (CSPDarkNet53) which is the modified version of DenseNet. CSPDarkNet-53 resolves the problem of vanishing gradients and empower the model learning through feature propagation, and re-usability. The CSPDarkNet-53 also reduces the hyperparameter of the network that ensures lower training latency

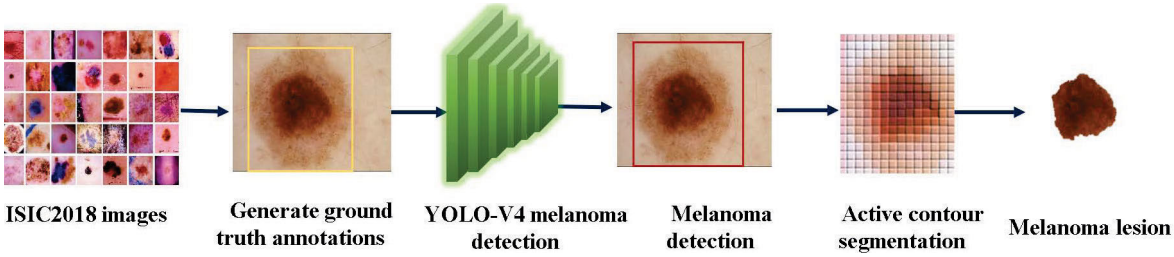

FIGURE 2. Melanoma lesion segmentation using melanoma localization and segmentation.

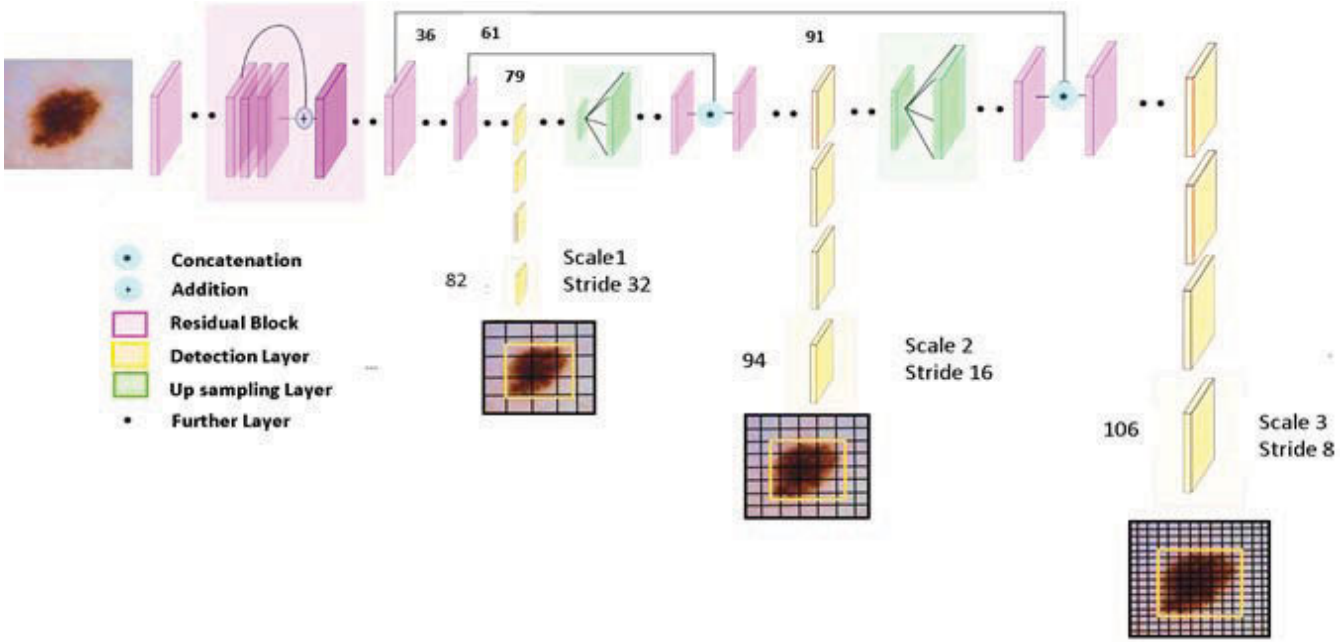

FIGURE 3. Melanoma lesion detection using YOLOv4 network.

and generates stronger decision boundaries. YOLOv4 was cascaded with Spatial Pyramid Pooling (SPP) block on top of CSPDarkNet-53 to enhance the deep receptive fields of melanoma contextual representation without increasing the computational overhead. The YOLOv4's neck aggregated the melanoma features using Path Aggregation Network (PANET) to enhance the discriminative ability of melanoma representation.

The YOLOv4 performed better melanoma localization due to additional optimization training strategies known as Bag of Freebies. The YOLOv4 ensures improvement in melanoma inference without increasing the hardware computations due to training YOLOv4 through Bag of Freebies. The YOLOv4 augmented the dermoscopy images with mosaic and cutmix augmentation and applied dropBlock regularization that improves the model learning. YOLOv4 generates the model for melanoma localization using self-adversarial training (SAT) with genetic algorithm for hyperparameter selection.

1) MELANOMA BOUNDING BOX PREDICTION

After model learning from YOLOv4, the test dermoscopic images are presented to YOLOv4 for localization and recognition of melanoma. YOLOv4 performs regression operation to estimate the location and recognition of melanoma class using contextual information of entire dermoscopic image in single pass, as illustrated in Fig 3. The YOLOv4 model divides the dermoscopic images into grids and in our work it is chosen as 7. YOLOv4's darknet model compute features of test dermoscopic image and generates the output feature map of size $n \times n \times (C + 1) + 5 \times k$, where $(C + 1)$ is the total number of classes including background class, and k is the number of anchors. As in our case we have only one class for recognition and detection that is melanoma, therefore currently the value of C is 1. However, the model can easily be tuned for detection of multiple disease. Therefore, the generic representation in the form of variable is used. The constant indicates the four offsets of bounding box i.e. x, y, height, width, and confidence score. The (x, y) coordinates represent

the center of the box relative to the grid cell. The width and height are predicted relative to the whole image.

The YOLOv4 design enables the end-to-end training and real-time processing with higher average precision rate. The YOLOv4 detect melanoma lesion when origin of ground truth mask T falls within $n \times n$ grid. Every grid is responsible to infer bounding boxes along with confidence score and melanoma class probability. The confidence prediction score C_f as described in the following Eq.(3) determine either region contain the melanoma or not.

$$C_f = p_m \times IoU_{pred}^{T}, \quad p_m \in \{0, 1\} \tag{3}$$

In case melanoma is inside the grid, the value of $p_m = 1$, otherwise $p_m = 0$, where p_m represents the probability of occurrence of melanoma. The IoU_{pred}^{T} represents the concurrence of melanoma lesion in predicted and ground truth T bounding box. The confidence score C_f measures the accurate detection of melanoma lesion. When multiple bounding boxes infer the presence of melanoma lesion across same region, then YOLOv4 select finest bounding box by applying a threshold overlapping score of 0.5. Moreover, for selecting precise bounding box across melanoma, The predicted melanoma lesion within the bounding boxes are weighted by melanoma predicted probabilities, which is essential in estimating the confidence score to improve true positive ratio.

E. MELANOMA SEGMENTATION USING ACTIVE CONTOUR

After melanoma lesion detection, the detected lesion is further processed to segment out the precise boundaries of melanoma using snake model of active contour segmentation [19]. The active contour segmentation technique estimates the pixel energy and segregate the pixels to generate a parametric contour having similar geometric characteristics. The contour model determines the preliminary outline to define the melanoma segments within the dermoscopic images by minimizing the energy function, as illustrated mathematically (4). Lower value of energy function is desirable for accurate description and regional analysis of melanoma lesion.

$$f_{energy} = min\{E_1, E_2, E_3, E_4\} \tag{4}$$

$$E_1(x, y) = \mu \int_{\Omega} \delta(\phi(x, y)) \, ||\nabla \phi(x, y)|| dxdy \tag{5}$$

$$E_2(x, y) = \nu \int_{\Omega} H(\phi(x, y)) \, dxdy \tag{6}$$

$$E_3(x, y) = \lambda_1 \int_{\Omega} ||\hat{D}(x, y) - c_1||^2 H(\phi(x, y)) \, dxdy \tag{7}$$

$$E_4(x, y) = \lambda_2 \int_{\Omega} ||u_0(x, y) - c_2||^2 (1 - H(\phi(x, y))) \, dxdy \tag{8}$$

where, f_{energy} minimizes the energy that is obtained by threshold function $\phi(x, y)$. The threshold function $\phi(x, y)$ is used to estimate whether melanoma lesion is inside or outside the contour C. The allows splitting of contour curve C towards the boundaries of melanoma. However, the entropy inside and outside the contour remains static. Here, $\hat{D}(x, y)$ is melanoma lesion detected by YOLOv4, as bounded by $\{\mu, \nu, \lambda_1, \lambda_2\} > 0$ with real numbers. The fitting weights are adjusted to identify precise boundaries. The Heaviside H and Dirac delta $\delta(.)$ functions are used to optimize the convergence of energy and c_1, c_2 are Mumford-Shah's segmentation models [20]. The snake model requires initial outline of melanoma lesion to identify similar neighboring regions. Therefore, prior knowledge of melanoma is significant for accurate estimation of melanoma boundaries by reducing energy function and finally for convergence to local minimum. To provide accurate initial estimate of melanoma contour, we reduce the detected bounding box coordinated by 10 pixels and generate a rectangular mask as initial contour. Snake model for melanoma segmentation passes the deformable model by energy minimization and dynamically coverage to the local minimum. The snake model for active contour is represented in (9).

$$C_v(s, t) = (x(s, t), y(s, t)) \tag{9}$$

The melanoma parametric curve $C_v(s, t)$ is exploited in snake model, which is the 2D curve representation of melanoma lesion with (x, y) coordinates, the curve is spline $C_v(s, t) \in [0, 1]$, s is linear $s \in [0, 1]$ and t is time parameter $t \in [0, \infty]$.

F. SIGNIFICANCE OF YOLOV4 AS MELANOMA DETECTOR

As ISIC-2018 and ISIC-2016 dermoscopic dataset are occluded with clinical and natural artifacts that adversely disrupt the precise segmentation of melanoma lesion. To mitigate the influence of occluded artifacts like black frame, blue ink marks, color chart and gel bubbles, within the dermoscopic images, we train our YOLOv4 model to consider these artifacts as background class along with normal skin region and melanoma lesion as another class. Therefore, our technique efficiently overcomes the occluded artifacts exhibited within ISIC-2016 and ISIC-2018 dermoscopic images and reduce the number of preprocessing steps. As, application of skin enhancement phase removes hair and clinical rule marks only, remaining artifacts including ink spots, gel bubbles, black frame, and color charts still disrupt the performance of segmentation. To mitigate the effect of remaining artefacts, YOLOv4 was trained to consider normal skin with remaining artifacts as background class. Moreover, YOLOv4 processes the complete dermoscopic image in single pass and does not generate region proposals that ensure fast localization of melanoma lesion. YOLOv4 predicts the location of melanoma lesion by estimating the class probabilities and generates a precise bounding box across the melanoma lesion (Fig 3). The elimination of region proposal phase in YOLOv4 also reduces the computational cost in contrast to the R-CNN, Fast RCNN and faster R-CNN object detectors.

III. EXPERIMENTS AND RESULTS

A. DATASETS

The proposed technique was evaluated on two open source benchmark datasets including, ISIC-2016 and ISIC-2018 dataset. These datasets are provided by International Symposium of Biomedical Imaging Collaboration (ISBI) for segmentation and recognition of melanoma [5]. For the segmentation task, ISIC-2016 consists of 900 training samples with corresponding ground truth masks and 379 test sample with corresponding ground truth test samples masks. Training and test samples ground truths are provided by the organizers for model learning and evaluation of segmentation technique. While, ISIC-2018 consists of 2594 training samples along with ground truth melanoma masks and 1000 test samples. However, ground truth masks for test sample are not available for evaluation. Therefore, we randomly divide the ISIC2018 data into 10:1 ratio so that 2334 and 260 samples are used as validation data.

B. EVALUATION METRICS

The performance of skin enhancement, localization and segmentation tasks was evaluated using peak signal to noise ratio(PSNR), structure similarity index(SSIM), intersection over union(IOU), mean average precision (mAP), dice score(D) and Jaccard index (J) evaluation measures.

1) SKIN ENHANCEMENT

To evaluate the performance of skin enhancement phase, we have estimated the peak signal to noise ratio (PSNR), and Structural Similarity Index (SSIM) to determine the quality of images after application of skin enhancement phase. The higher PSNR value depicts that the quality of an image is retained and it must be greater than 20dB. The mathematical representation of PSNR is illustrated as

$$PSNR = -20 \times log_{10}\left(\frac{I_s}{MSE}\right) \tag{10}$$

The structural similarity index quantifies the resultant enhanced image in terms of luminance, contrast and the structural representation of image. For an input noisy and refined image the overall equation for SSIM is defined as:

$$SSIM\,(I, I_s) = \left[l\,(I, I_s)^{\alpha}\,.c\,(I, I_s)^{\beta}\,.s\,(I, I_s)^{\gamma}\right] \tag{11}$$

where

$$l\,(I, I_s) = \frac{2\mu_I\mu_{I_s} + C_1}{\mu_I^2 + \mu_{I_s}^2 + C_1}, \tag{12}$$

$$c\,(I, I_s) = \frac{2\sigma_x\sigma_y + C_2}{\sigma_x^2 + \sigma_y^2 + C_2}, \tag{13}$$

$$s\,(I, I_s) = \frac{\sigma_{II_s} + C_3}{\sigma_I\sigma_{I_s} + C_3}, \tag{14}$$

where $C_1 = (0.01 * L)^2$, $C_2 = (0.03 * L)^2$, $C_3 = C_2/2$, and $\mu_x, \mu_y, \sigma_x, \sigma_y, \sigma_{xy}$ represent means, standard deviations, and cross-covariance among the input noisy and refined images, and L is intensity level. The SSIM value lies between 0 and 1 and for better enhancement, its value should be very close to 1.

2) MELANOMA DETECTION

YOLOv4 performs detection of Melanoma skin cancer using intersection-over-union (IOU) which determines the similarity of ground truth box with a predicted box of melanoma lesion region. For the proposed detection model, IOU threshold was set to 0.6. If the IOU is greater than 0.6, then the prediction of melanoma is truly positive or correct otherwise it is considered as false positive.

$$IOU = 2.\frac{TP}{FN + TP + FP} \tag{15}$$

For evaluation of localization phase, precision and recall are most generally used evaluation metrics. The precision measures the fraction of positive predictions that are correct by dividing the number of correct positives found over the total amount of detections. The recall measures the fraction of correct positive predictions out of all actual positive entries. Precision and recall are defined as follows:

$$mAP = \frac{TP}{TP + FP} \tag{16}$$

Here, the TP, FP, and FN represent True Positive, False Positive, and False Negative, respectively.

3) MELANOMA SEGMENTATION

To evaluate segmentation performance, we have used the challenge evaluation metrics that include specificity (SP), sensitivity (SE), accuracy (Ac), Dice score (D) and Jaccard coefficient (J). First, we calculated these measures for an individual image then we take the average for the entire testing images for the final result. The above-mentioned criteria are described as:

$$SP = \frac{TP}{TP + FP} \tag{17}$$

$$SE = \frac{TP}{TP + FN} \tag{18}$$

$$A = \frac{TP + TN}{TP + TN + FP + FN} \tag{19}$$

$$D = \frac{2.TP}{2TP + FP + FN} \tag{20}$$

$$J = \frac{TP}{TP + FP + FN} \tag{21}$$

where TP, TN, FP, and FN denote True Positive, True Negative, False Positive, and False Negative, respectively. If melanoma lesion area is present and it is detected then it is considered as true positive and if it's not detected then it is regarded as a false negative. However, if a healthy skin area is detected as a healthy region then it is considered as true negative otherwise it is a false positive.

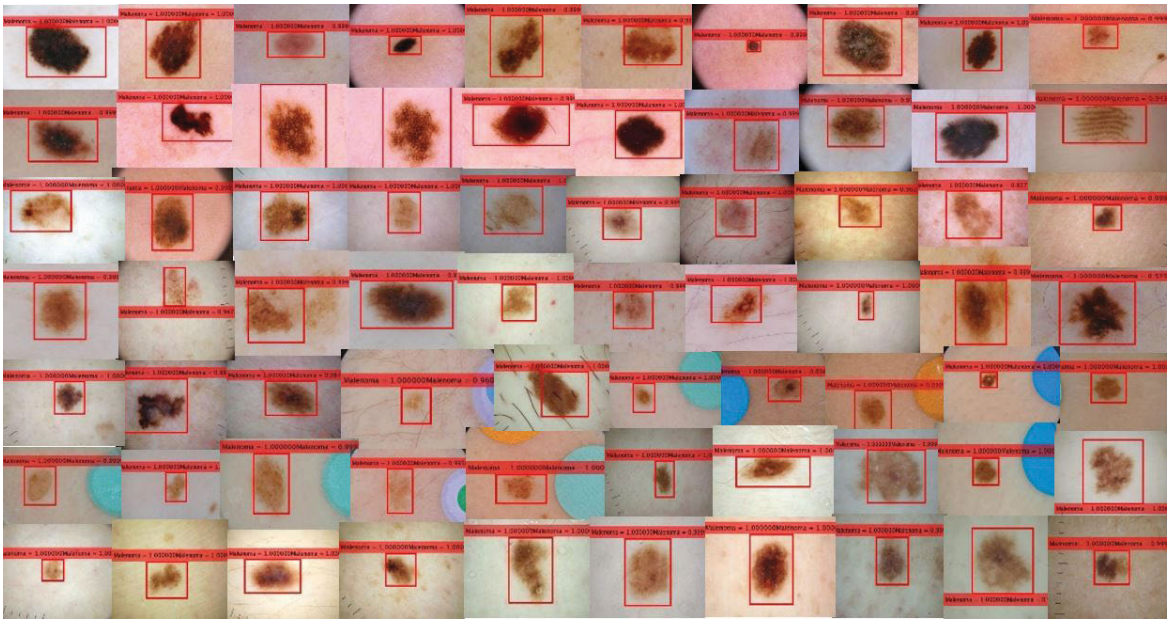

FIGURE 4. High melanoma confidence scoring test samples of ISIC2018 and ISIC2016 datasets, selected from highest scoring localization phase.

TABLE 1. Evaluation of skin enhancement phase using SSIM and PSNR measures.

Dataset	Artifacts					
	Thick hair		Thin hair		Rule marks	
	PSNR	SSIM	PSNR	SSIM	PSNR	SSIM
ISIC-2016	32.98	0.97	45.23	0.95	39.88	0.96
ISIC-2018	29.78	0.95	36.45	0.98	38.99	0.97

C. EXPERIMENTAL RESULTS

1) SKIN ENHANCEMENT

As discussed earlier, dermoscopic images of ISIC2016 and ISIC2018 dataset are disrupted by hair, color charts, gel bubble, ink or clinical rule marks. The segmentation performance of the proposed algorithm degrades in presence of these artifacts, therefore skin enhancement phase is applied to mitigate the artifact's occlusions to improve the performance of melanoma lesion segmentation. We evaluate the performance of skin enhancement phase using structural similarity index (SSIM) and peak signal to noise ratio(PSNR) among original and skin enhanced dermoscopic images. The observed results are illustrated in Table 1.

The PSNR and SSIM values are presented in Table 1. The obtained PSNR and SSIM values ensures slight loss in image information on application of skin enhancement phase. Such small information loss does not affect the segmentation performance. Rather, the skin enhancement phase improves the quality of image by removing the unnecessary artifacts. It is notable from Table 1 that PSNR measure is higher than 29db, while SSIM is higher than 0.9. This validates that structural, intensity and chrominance factors remain sustained after skin enhancement phase. Our skin enhancement phase removes hair, clinical rule marks only, as shown in Fig 5. While, rest of artifact are modeled as non-melanoma lesion using YOLOv4.

2) ABLATION STUDY ON YOLO DETECTOR FAMILY

We performed an ablation study on all the variants of YOLO family to select the optimal melanoma detector. Melanoma detection is challenging task due to obscure melanoma boundaries and wide variations in texture and colour of melanoma. Therefore, we kept the similar experimental setting and examined the impact of variants of YOLO for melanoma localization.

The incremental development of YOLO family members differs in technical aspects of backbone network, neck and head part of the detector that make the newer version more decisive than previous, as illustrated in Table 2. The initial version of YOLO v1 [21] used end-to-end differentiable backbone network of 24-layered CNN model. While, YOLOv2 [22] used DarkNet19 as a backbone model with batch normalization, and anchor boxes. The neck and head part in YOLOv1 and YOLOv2 was based on

TABLE 2. Evaluation of YOLO family variants for melanoma localization.

YOLO	Backbone	Neck	Head	mAP
v1	24-layered CNN	NM suppression	Softmax	0.37
v2	DarkNet-19	NM suppression	Softmax	0.83
v3	DarkNet-53	FPN	Log. regr	0.93
v4	CSPDarknet53	PANET	YOLOv3	0.97
v5	CSPDarknet53	PANET	YOLOv3	0.97

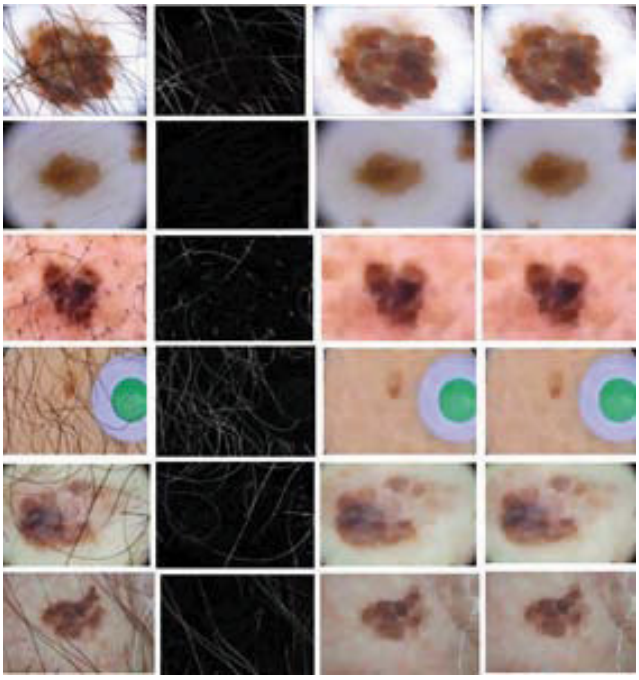

FIGURE 5. Skin enhancement phase for removing the artefacts and improving the quality of dermoscopic images. Column I presents the occluded original input image with artefacts including, hair, black frame, color charts, etc., column II presents hair artefact mask which was removed by morphological closing operation, column III presents the resultant outcome of morphological operation and column IV presents the sharper enhanced dermoscopic image after application of sharpening operation.

non-maximal(NM) suppression and Softmax layer for prediction and localization of melanoma.

The YOLOv3 [23] detector was developed to make the melanoma prediction with objectness score to be more assertive in prediction of melanoma lesion. The YOLOv3's neck part includes Feature Pyramid Network (FPN) to aggregate the deep feature maps of backbone network DarkNet-53. This aggregation of feature maps at three different levels of pyramid allows granularity to cater the detection of smaller melanoma lesion.

The latest YOLOv4 version performed better than previous YOLO versions for melanoma detection due to technical improvements at backbone network, neck and head part of detector. The ablation study portray that YOLOv4 performed better in melanoma localization due to additional optimization training strategies known as Bag of Freebies. YOLOv4 generates the model for melanoma localization using self-adversarial training (SAT) with genetic algorithm for hyperparameter selection. YOLOv5 adapts YOLOv4 in pytorch that reduces the training and inferencing time. However, the melanoma localization performance of YOLOv4 and YOLOv5 is comparable. This experiment suggests to use YOLOv4 for melanoma localization with CSPDarkNet53 as backbone Network and SSP block to obtain contextual melanoma representation with PANet for feature aggregation.

The empirical findings of ablation study on various variants of YOLO illustrate that optimal choice of YOLO detector is YOLOv4. As the YOLOv4 generates stronger decision boundaries to localize and recognize melanoma lesion.

3) MELANOMA LOCALIZATION USING YOLOv4

After skin enhancement phase, dermoscopic images are processed by YOLOv4 for localization of melanoma lesion based on the emperical findings of ablation studies. YOLOv4 was trained to discriminate between the melanoma lesion and normal skin pixel at 20k steps. YOLOv4 fuses low-level and high-level features for better prediction of regions and maps predicted lesion in accordance with the trained model to classify among normal or melanoma lesion. Yolov4 considers melanoma as positive class and normal skin with artifacts as negative class. The IoU threshold for melanoma detection was chosen as 0.9, while IoU lower than 0.9 is considers as normal skin patch. YOLOv4 localized melanoma lesion with prediction confidence score through logistic regression. At 20K steps, YOLOv4 weights are tuned to discriminate melanoma and normal skin with lower prediction loss as results are shown in Table 3. From the Table 3, it is notable that YOLOv4 localizes the melanoma lesion with commendable mean average precision (mAP) and overcomes the artifacts like color clinical chart, black frame, gel bubble, hair and clinical rule marks. Few high scoring detection results are illustrated, in Fig 4. YOLOv4 is capable to identify melanoma at multiple scale and orientation despite of skin color variation (Fig 4).

TABLE 3. Mean average precision and processing time required to localize melanoma.

ISIC2016 Artefacts	mAP	Time (msec)	ISIC2018 Artefacts	mAP	Time
Thick Hair	0.99	50.1	Thick Hair	0.95	50.3
Think Hair	0.98	52.1	Think Hair	0.98	52.4
Rule marks	0.97	52.3	Rule marks	0.95	54.6
Color charts	0.99	49.45	Color charts	0.97	50.8
Black frame	0.99	51.9	Black frame	0.98	52.4

4) MELANOMA SEGMENTATION

To estimate the performance of melanoma lesion segmentation, a precise melanoma boundary area is needed. After melanoma localization, the localized region is processed further to obtain boundary of melanoma lesion through active contour segmentation. The active contour segmentation segregates the melanoma lesion using region growing of snake model and resultant images are approximately similar to actual melanoma region, as illustrated in Fig 5, column IV. The segmentation phase is evaluated using Ac, SE, and SP at pixel level. The proposed technique achieved averaged

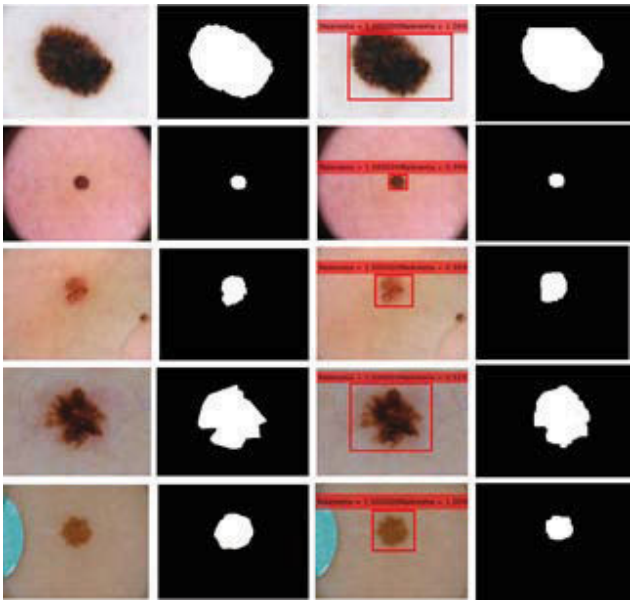

FIGURE 6. Column I presents the original skin enhanced dermoscopic images of ISIC2018 and ISIC2016 dataset, Column II presents the corresponding ground truth masks of melanoma lesion, Column III presents the YOLOv4 localized melanoma lesion, and Column IV presents the segmented melanoma lesion using active contour segmentation.

score of Ac as 0.95, SE as 0.932, and SP as 0.9345 on ISIC2018 dataset. Where, J and D score were observed for all the test samples and average scores are reported as 0.98 and 0.89 on ISIC 2018. Similarly, for ISIC2106 recorded average A as 0.93, SE as 0.94, and SP as 0.952. Where, J and D score were observed for all the test samples and average scores are 0.96 and 0.92. We attribute localization of melanoma lesion as reason behind the efficient and robust performance of our method. YOLOv4 precisely identifies the melanoma lesion in 50ms and considers artifacts as background region. Applying active contour segmentation only on detected region is effective in improving the segmentation performance of our proposed technique.

5) COMPARISON WITH CHALLENGE PARTICIPANTS

At ISBI 2016 challenge for melanoma segmentation task, twenty eight teams participated and presented the results of their technique, as listed in Table 4. The ISBI ranked the participants of segmentation according to the highest average J score. From the results reported in Table 4, it is notable that all the top ten participants of segmentation phase have used deep learning algorithm due to precise segmentation and effective backpropagation learning to reduce the segmentation error. Moreover, participants of ISIC2016 have used pretrained shallower models including ALEXNET [24], VGG16 [25] and Resnet [26] to estimate the precise boundaries of melanoma lesion. Our proposed technique overcomes the challenges of ISIC2016 datasets and achieved highest J score which is better than all of the participants. However, EXB applied pre-processing and post processing steps to improve the segmentation results and ExB's Jaccard score is highest among the top ten participants of ISIC2016. CUMED the second runner up in ISIB segmentation task, employed fully convolutional residual network (FCRN). CUMED framework was end-to-end deep network without pre-processing or post processing.

TABLE 4. Performance comparison with top ten participants of ISIB 2016 melanoma segmentation task.

Method	A	D	J	SE	SP
ExB	0.95	0.91	0.84	0.91	**0.965**
CUMED	0.94	0.897	0.829	0.911	0.957
Mahmudur	0.952	0.895	0.822	0.88	0.969
SFU-mial	0.944	0.885	0.811	0.915	0.955
TMUteam	0.946	0.888	0.81	0.832	0.987
UiT-Seg	0.939	0.881	0.806	0.863	0.974
IHPC-CS	0.938	0.879	0.799	0.91	0.941
UNIST	0.94	0.867	0.797	0.876	0.954
Jose Luis	0.934	0.869	0.791	0.87	0.978
Marco romelli	0.936	0.864	0.786	0.883	0.962
Proposed	**0.939**	**0.92**	**0.96**	**0.942**	0.952

While comparing the segmentation results with top ten participants of ISIB2016, it validates that the proposed approach perform better than top ten participants. Our proposed method scores highest J, D, A and SE. However, ExB[3] SP is 0.013 times higher than our SP. The reason behind the good performance of our method stems from precise localization of melanoma lesion before application of segmentation phase. We believe that artifacts within the dermoscopic images of ISIC2016 degraded the segmentation performance. As discussed earlier, our YOLOv4 [1] detector was trained to consider artifacts as background and it localizes the precise melanoma lesion. In our proposed approach active contour segmentation was applied only on melanoma detected region instead of entire dermoscopic image. Therefore, our segmentation results are better than top ten participants of ISBI challenge.

6) COMPARISON WITH STATE-OF-THE-ART TECHNIQUES

To further evaluate the performance of our proposed approach for melanoma segmentation, we compared our method with state-of-the art segmentation techniques, as represented in Table 5. Traditional approaches for melanoma segmentation including, active contour, bootstrapping [15], contextual hypergraph [14], clustering [27], region split and merge, region growing [8], sparse coding [28] and thresholding techniques [7] produce lower value of average J score than our method. This is due to the fact that these approaches segment the melanoma lesion based on spatial context information in unsupervised fashion. While our proposed approach initially builds a model based on high level color, texture and spatial representation of melanoma. Therefore, at test time, trained

TABLE 5. Performance evaluation of proposed method with state-of-the-art techniques.

Technique	A	D	J	SP	Time
Adaptive thresholding [7]	0.72	0.56	0.45	0.8	2
Bootstrap learning [15]	0.78	0.72	0.57	0.75	-
Contextual hypergraph [14]	0.83	0.75	0.6	0.78	0.3
ISO [9]	0.82	0.68	0.56	0.77	-
Level set [29]	0.7	0.58	0.46	0.79	0.84
Sparse coding [28]	0.91	0.8	0.67	0.86	0.1
Region growing [13]	0.73	0.55	0.43	0.76	0.4
Yen's thresholding [30]	0.81	0.67	0.58	0.77	-
FCN [31]	0.82	0.82	0.86	0.7	0.05
Segnet [32]	0.91	0.92	0.86	0.96	0.06
PSPN [33]	0.85	0.86	0.84	0.85	0.79
DeepLab-v3 [34]	0.87	0.85	0.84	0.85	0.89
Proposed	**0.94**	**0.92**	**0.96**	0.94	0.01

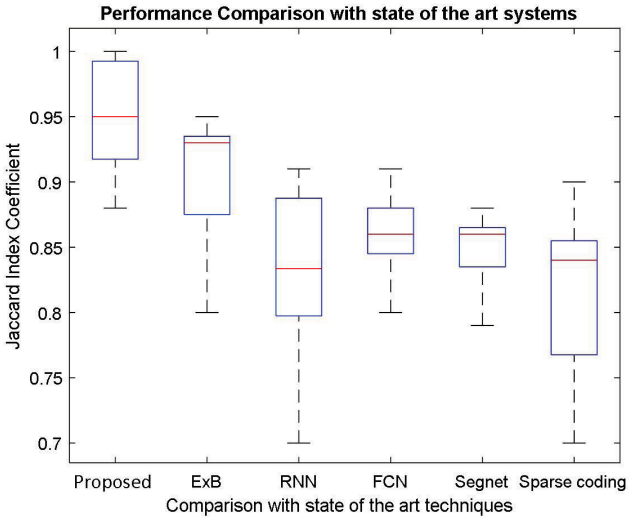

FIGURE 7. Box and whisker plot to represent the spread of Jaccard score in contrast state-of-the-art techniques.

model localized melanoma lesion with high mAP and only detected region is considered for segmentation.

Beside traditional techniques for segmentation, deep learning-based approaches i.e., FCN [31], and Segnet [32], performed melanoma segmentation with J score of 0.86. The FCN requires feature maps as input to learn the semantic representation of melanoma by processing through the convolutional and pooling layers. As the FCN [31] and Segnet [32] used a deeper network for segmentation of melanoma lesions, therefore the training model required tuning of thousands of hyperparameters, which makes the melanoma segmentation computationally expensive. Other deep learning based segmentation approaches i.e., PSPN [33] understands the contextual information of melanoma lesion and extract deep receptive fields to learn the global-scene-level melanoma prior. Whereas, the DeepLab model [34] used atrous convolutions and atrous spatial pyramid pooling (ASPP) for melanoma segmentation. The DeepLab model extracts deep features from backbone ResNet101 network and atrous convolution to adjust the dermoscopy image to same resolution as provided at input stage. The DeepLab's ASPP network performs classification at pixel level to recognize melanoma lesion [34]. The PSPN and DeepLab V3 segmentation results are comparable with proposed YOLO V4 model with active contour segmentation for melanoma segmentation.

It is justified from Table 5 that our method exhibits lower computational time with precise melanoma segmentation in contrast to state-of-the-art methods. Our Jaccard score is 0.10% higher than Segnet [32] due to the training of YOLOv4 to consider clinical and natural artifacts as background region and only detect the melanoma lesion in single pass. We have applied a simple morphological operation for blood vessels and hair removal. The reason behind application of simple preprocessing technique is due to the fact the YOLOv4 is powerful enough to overcome the all the diverse artifacts and build a decision boundary to predict melanoma region. Here, we emphasize that YOLOv4 is not only used for melanoma localization but also for considering clinical or natural artifacts as non-melanoma lesion.

The problem of precise melanoma detection is challenging due to visual similarity with normal skin lesion. Moreover, the boundaries of melanoma lesion is irregular and this non uniformity of shape and heterogeneous nature of melanoma makes the detection of melanoma lesion challenging. Moreover, there is huge variation in texture and color of melanoma lesion that confuses the dermatologist to accurately predict the melanoma. However, earlier diagnosis is essential to medicate the patient timely and stop the prognosis of disease. Deep learning tools like YOLOv4 with active contour segmentation empowers the CAD solutions to precisely detect the melanoma lesion and improve the patient life expectancy.

We plotted boxplot to examine the distribution of obtained J Jaccard score of test samples and compared the performance of FCN [31], Segnet [32], ExB [4] and RNN [17] with our proposed technique. The spread of box and whisker plot signify that more than 50% of our predicted Jaccard scores lies within the range of 0.93-0.98 and entire test samples' Jaccard scores appeared within 0.87-0.98 which is higher than state-of-the-art methods. Moreover, the median of our proposed method lies at 0.95 which validates the effectiveness of proposed scheme. Similarly, median Jaccard index of [32] and [31] appeared at 0.86. Thus, preprocessing followed by YOLOv4 [1] and Active contour segmentation meaningfully improves the segmentation and localization of melanoma as compared to state-of-the-art techniques.

IV. CONCLUSION

In this article, we presented a novel scheme for melanoma localization and segmentation using YOLOv4 and active

contour segmentation. Our proposed framework consists of three phases: skin enhancement, melanoma localization and finally melanoma segmentation. Our proposed method efficiently and precisely detects and segments the melanoma lesion in contrast to state-of-the-art methods. YOLOv4 empowers our scheme to recognize various kinds of skin diseases precisely and efficiently. The proposed method can further be utilized in other medical image segmentation problems.

REFERENCES

[1] A. Bochkovskiy, C.-Y. Wang, and H.-Y. M. Liao, "YOLOv4: Optimal speed and accuracy of object detection," 2020, *arXiv:2004.10934*. [Online]. Available: http://arxiv.org/abs/2004.10934

[2] A. Esteva, B. Kuprel, R. A. Novoa, J. Ko, S. M. Swetter, H. M. Blau, and S. Thrun, "Dermatologist-level classification of skin cancer with deep neural networks," *Nature*, vol. 542, no. 7639, pp. 115–118, Feb. 2017.

[3] N. Razmjooy, F. R. Sheykhahmad, and N. Ghadimi, "A hybrid neural network–world cup optimization algorithm for melanoma detection," *Open Med.*, vol. 13, no. 1, pp. 9–16, Mar. 2018.

[4] L. Yu, H. Chen, Q. Dou, J. Qin, and P.-A. Heng, "Automated melanoma recognition in dermoscopy images via very deep residual networks," *IEEE Trans. Med. Imag.*, vol. 36, no. 4, pp. 994–1004, Apr. 2017.

[5] N. Nida, A. Irtaza, A. Javed, M. H. Yousaf, and M. T. Mahmood, "Melanoma lesion detection and segmentation using deep region based convolutional neural network and fuzzy C-means clustering," *Int. J. Med. Informat.*, vol. 124, pp. 37–48, Apr. 2019.

[6] V. Rajinikanth, N. S. Madhavaraja, S. C. Satapathy, and S. L. Fernandes, "Otsu's multi-thresholding and active contour snake model to segment dermoscopy images," *J. Med. Imag. Health Informat.*, vol. 7, no. 8, pp. 1837–1840, Dec. 2017.

[7] M. Silveira, J. C. Nascimento, J. S. Marques, A. R. S. Marcal, T. Mendonca, S. Yamauchi, J. Maeda, and J. Rozeira, "Comparison of segmentation methods for melanoma diagnosis in dermoscopy images," *IEEE J. Sel. Topics Signal Process.*, vol. 3, no. 1, pp. 35–45, Feb. 2009.

[8] A. Wong, J. Scharcanski, and P. Fieguth, "Automatic skin lesion segmentation via iterative stochastic region merging," *IEEE Trans. Inf. Technol. Biomed.*, vol. 15, no. 6, pp. 929–936, Nov. 2011.

[9] T. W. Ridler and S. Calvard, "Picture thresholding using an iterative selection method," *IEEE Trans. Syst., Man, Cybern.*, vol. TSMC-8, no. 8, pp. 630–632, Aug. 1978.

[10] T. Wadhawan, N. Situ, K. Lancaster, X. Yuan, and G. Zouridakis, "SkinScan: A portable library for melanoma detection on handheld devices," in *Proc. IEEE Int. Symp. Biomed. Imag., Nano Macro*, Mar. 2011, pp. 133–136.

[11] A. Masood and A. A. Jumaily, "Fuzzy C mean thresholding based level set for automated segmentation of skin lesions," *J. Signal Inf. Process.*, vol. 4, no. 3, p. 66, 2013.

[12] J. F. Alcon, C. Ciuhu, W. T. Kate, A. Heinrich, N. Uzunbajakava, G. Krekels, D. Siem, and G. de Haan, "Automatic imaging system with decision support for inspection of pigmented skin lesions and melanoma diagnosis," *IEEE J. Sel. Topics Signal Process.*, vol. 3, no. 1, pp. 14–25, Feb. 2009.

[13] M. E. Celebi, H. A. Kingravi, H. Iyatomi, Y. Alp Aslandogan, W. V. Stoecker, R. H. Moss, J. M. Malters, J. M. Grichnik, A. A. Marghoob, H. S. Rabinovitz, and S. W. Menzies, "Border detection in dermoscopy images using statistical region merging," *Skin Res. Technol.*, vol. 14, no. 3, pp. 347–353, Aug. 2008.

[14] X. Li, Y. Li, C. Shen, A. Dick, and A. V. D. Hengel, "Contextual hypergraph modeling for salient object detection," in *Proc. IEEE Int. Conf. Comput. Vis.*, Dec. 2013, pp. 3328–3335.

[15] N. Tong, H. Lu, X. Ruan, and M.-H. Yang, "Salient object detection via bootstrap learning," in *Proc. IEEE Conf. Comput. Vis. Pattern Recognit. (CVPR)*, Jun. 2015, pp. 1884–1892.

[16] Y. Yuan, M. Chao, and Y.-C. Lo, "Automatic skin lesion segmentation using deep fully convolutional networks with Jaccard distance," *IEEE Trans. Med. Imag.*, vol. 36, no. 9, pp. 1876–1886, Sep. 2017.

[17] M. Attia, M. Hossny, S. Nahavandi, and A. Yazdabadi, "Skin melanoma segmentation using recurrent and convolutional neural networks," in *Proc. IEEE 14th Int. Symp. Biomed. Imag. (ISBI)*, Apr. 2017, pp. 292–296.

[18] M. A. Al-Masni, M. A. Al-Antari, M.-T. Choi, S.-M. Han, and T.-S. Kim, "Skin lesion segmentation in dermoscopy images via deep full resolution convolutional networks," *Comput. Methods Programs Biomed.*, vol. 162, pp. 221–231, Aug. 2018.

[19] T. McInerney and D. Terzopoulos, "Deformable models in medical image analysis: A survey," *Med. Image Anal.*, vol. 1, no. 2, pp. 91–108, Jun. 1996.

[20] X. Bresson, S. Esedoğlu, P. Vandergheynst, J.-P. Thiran, and S. Osher, "Fast global minimization of the active contour/snake model," *J. Math. Imag. Vis.*, vol. 28, no. 2, pp. 151–167, Aug. 2007.

[21] J. Redmon, S. Divvala, R. Girshick, and A. Farhadi, "You only look once: Unified, real-time object detection," in *Proc. IEEE Conf. Comput. Vis. Pattern Recognit. (CVPR)*, Jun. 2016, pp. 779–788.

[22] J. Redmon and A. Farhadi, "YOLO9000: Better, faster, stronger," in *Proc. IEEE Conf. Comput. Vis. Pattern Recognit. (CVPR)*, Jul. 2017, pp. 7263–7271.

[23] J. Redmon and A. Farhadi, "YOLOv3: An incremental improvement," 2018, *arXiv:1804.02767*. [Online]. Available: http://arxiv.org/abs/1804.02767

[24] A. Krizhevsky, I. Sutskever, and G. E. Hinton, "Imagenet classification with deep convolutional neural networks," in *Proc. Adv. Neural Inf. Process. Syst.*, 2012, pp. 1097–1105.

[25] K. Simonyan and A. Zisserman, "Very deep convolutional networks for large-scale image recognition," 2014, *arXiv:1409.1556*. [Online]. Available: http://arxiv.org/abs/1409.1556

[26] K. He, X. Zhang, S. Ren, and J. Sun, "Deep residual learning for image recognition," in *Proc. IEEE Conf. Comput. Vis. Pattern Recognit. (CVPR)*, Jun. 2016, pp. 770–778.

[27] Z. Zhao, T. Bouwmans, X. Zhang, and Y. Fang, "A fuzzy background modeling approach for motion detection in dynamic backgrounds," in *Proc. Int. Conf. Multimedia Signal Process.* Shanghai, China: Springer, 2012, pp. 177–185.

[28] B. Bozorgtabar, M. Abedini, and R. Garnavi, "Sparse coding based skin lesion segmentation using dynamic rule-based refinement," in *Proc. Int. workshop Mach. Learn. Med. Imag.* Athens, Greece: Springer, 2016, pp. 254–261.

[29] C. Li, C.-Y. Kao, J. C. Gore, and Z. Ding, "Minimization of region-scalable fitting energy for image segmentation," *IEEE Trans. Image Process.*, vol. 17, no. 10, pp. 1940–1949, Oct. 2008.

[30] M. Sezgin and B. Sankur, "Survey over image thresholding techniques and quantitative performance evaluation," *J. Electron. Imag.*, vol. 13, no. 1, pp. 146–166, 2004.

[31] J. Long, E. Shelhamer, and T. Darrell, "Fully convolutional networks for semantic segmentation," in *Proc. IEEE Conf. Comput. Vis. Pattern Recognit. (CVPR)*, Jun. 2015, pp. 3431–3440.

[32] V. Badrinarayanan, A. Handa, and R. Cipolla, "SegNet: A deep convolutional encoder-decoder architecture for robust semantic pixel-wise labelling," 2015, *arXiv:1505.07293*. [Online]. Available: http://arxiv.org/abs/1505.07293

[33] H. Zhao, J. Shi, X. Qi, X. Wang, and J. Jia, "Pyramid scene parsing network," in *Proc. IEEE Conf. Comput. Vis. Pattern Recognit. (CVPR)*, Jul. 2017, pp. 2881–2890.

[34] L.-C. Chen, G. Papandreou, F. Schroff, and H. Adam, "Rethinking atrous convolution for semantic image segmentation," 2017, *arXiv:1706.05587*. [Online]. Available: http://arxiv.org/abs/1706.05587

SALEH ALBAHLI received the B.Sc. degree from Qassim University, Saudi Arabia, in 2005, the M.I.T. degree from the University of Newcastle, Australia, in 2010, and the Ph.D. degree from Kent State University, USA, in 2016, all in computer science. He is currently an Associate Professor with the College of Computer, Qassim University. His research interests include databases technology especially as they relate to semantic web technologies and the integration of semantic web in database systems, big data analytic, data science, and machine learning. He has attended various conferences, symposiums, workshops, training, and presented many seminars. He has over 15 years of experience in both IT industry and academia in Saudi Arabia, Australia, and USA.

NUDRAT NIDA received the B.Sc. and M.Sc. degrees in computer engineering from the University of Engineering and Technology at Lahore, Pakistan, and the Ph.D. degree from UET at Taxila, in 2016. She is currently a Lecturer with Air University, Aerospace and Aviation Campus, Kamra, Pakistan. Her research interests include video analytics, automated action recognition, automated behavior analysis, and biomedical image analysis.

AUN IRTAZA received the Ph.D. degree from FAST-nu, Islamabad, Pakistan, in 2016. During his Ph.D. degree, he remained working as a Research Scientist with the Gwangju Institute of Science and Technology (GIST), South Korea. He became an Associate Professor with the University of Engineering and Technology (UET) at Taxila, Taxila, Pakistan, in 2017, where he became the Chair of the Department of Computer Science, in 2018. He has more than 40 publications in IEEE, Springer, and Elsevier journals. He is currently working as a Visiting Associate Professor with the University of Michigan at Dearborn, Dearborn. His research interests include computer vision, multimedia forensics, audio-signal processing, medical image processing, and big data analytics.

MUHAMMAD HAROON YOUSAF (Senior Member, IEEE) is currently serving as an Associate Professor with the Computer Engineering Department, University of Engineering and Technology at Taxila, Taxila, Pakistan. He is the Head of the Swarm Robotics Laboratory under the National Centre for Robotics and Automation. He has published more than 50 papers in International Conferences and Journals. His research interests include image processing and computer vision. He has been serving as a TPC member for many conferences and a Reviewer for renowned journals. He is a Professional Member of the Pakistan Engineering Council. He was a recipient of the Best University Teacher Award (from 2012 to 2013) given by the Higher Education Commission (HEC) of Pakistan.

MUHAMMAD TARIQ MAHMOOD (Senior Member, IEEE) received the M.C.S. degree in computer science from the AJK University of Muzaffarabad, Pakistan, in 2004, the M.S. degree in intelligent software systems from the Blekinge Institute of Technology, Sweden, in 2006, and the Ph.D. degree in information and mechatronics from the Gwangju Institute of Science and Technology, South Korea, in 2011. He is currently serving as an Associate Professor with the School of Computer Science and Engineering, Korea University of Technology and Education, South Korea. His research interests include image processing, 3D shape recovery, computer vision, and machine learning.